Available online at www.sciencedirect.com

ScienceDirect

journal homepage: www.elsevier.com/locate/jtte

Original Research Paper

Two methodological approaches to assess the seismic vulnerability of masonry bridges

Diego Maria Barbieri [a,b,*]

[a] *Department of Civil and Environmental Engineering, Norwegian University of Science and Technology, Trondheim 7491, Norway*

[b] *Department of Civil, Constructional and Environmental Engineering, Sapienza University of Rome, Rome 00184, Italy*

HIGHLIGHTS

- Deterministic and probabilistic approaches for seismic vulnerability assessment.
- Fragility curves represent useful descriptions of seismic damage scenarios.
- Fragility curves are effective tools for the railway network asset management.
- In-situ investigation comprising more than one hundred masonry arch bridges.
- Structural parameters comparison between Eurocode and in-situ investigation.

ARTICLE INFO

Article history:
Received 19 May 2018
Received in revised form
11 September 2018
Accepted 13 September 2018
Available online 8 December 2018

Keywords:
Railway masonry arch bridge
Bridge maintenance and conservation
Masonry mechanical parameters
Non-linear static analysis
Seismic fragility
Finite element analysis

ABSTRACT

This work describes the seismic vulnerability assessment of a railway masonry arch bridge. Its conservation state is initially investigated by means of a thorough field and laboratory test campaign, comprising destructive and non-destructive tests. Two different methods are used to evaluate the bridge seismic vulnerability. The first method adopts a deterministic approach and corresponds to a single non-linear static analysis, performed as described in the Eurocodes. The second method employs a probabilistic approach and considers the variability of the involved mechanical parameters (structure geometry and properties of the building materials) and seismic parameters (intensity of the action and site conditions). This method associates the probabilistic values of ground acceleration exceedance to the estimated seismic vulnerability. This is shown by means of fragility curves, which allow to take into consideration the uncertainty of the various components involved in the definition of the seismic vulnerability and display the seismic damage scenarios. Currently no code requires to perform this calculation procedure. In addition, this work compares the values of masonry mechanical properties specified in the Eurocodes with those obtained in an extensive investigation campaign involving more than one hundred masonry bridges. Compressive strength and longitudinal elasticity modulus are the relevant mechanical parameters investigated. The outcomes of this research can contribute to the development of a more efficient maintenance system of the masonry bridges belonging to the railway network. This has an important role when it comes to establishing the priority order of assets intervention.

* Corresponding author. Department of Civil and Environmental Engineering, Norwegian University of Science and Technology, Norway. Tel.: +47 93002908; fax: +47 73 59 70 21.
E-mail addresses: diego.barbieri@ntnu.no, diegomb271@gmail.com.

Peer review under responsibility of Periodical Offices of Chang'an University.
https://doi.org/10.1016/j.jtte.2018.09.003

1. Introduction and background

Modern masonry bridges, and especially railway bridges, were mainly built between the mid-1800s and early 1900s. Many of them were placed on major railway lines crossing seismic areas and were designed before the introduction of seismic codes (Varum et al., 2011). The masonry bridges belonging to the Italian railway were built according to the typologies and instructions specified by the Railway Manual of Practice (Italian Railway Network, 1907).

Nowadays, there are roughly 200,000 railway bridges in operation in Europe, more than 40% are represented by masonry arch bridges (Paulsson et al., 2008). The Italian railway network consists of about 16,000 km line and approximately has 56,400 bridges; they are made of different materials as depicted in Fig. 1(a). The total length of railway line lying on masonry arches is about 450 km (Cocciaglia and Mosca, 1998); these structures vary from short single-span bridges to long multi-span viaducts, as shown in Fig. 1(b).

Italy offers a rich heritage of bridge structures because of the territory characterized by arduous orographic conditions. Being among the oldest infrastructures built in the country, masonry bridges represent a challenging issue when it comes to their maintenance. The structures must be in suitable condition to allow the normal rail traffic with the required safety level at all times (Union Internationale des Chemins de fer (UIC), 2009a, b). Managing authorities' goal is to optimize the available economical and material resources to identify the most critical structures and adopt possible rehabilitation measures (Modena et al., 2015; Tecchio et al., 2012; Zampieri et al., 2018b). Scheduled maintenance and seismic assessment of the network assets are necessary to guarantee complete serviceability. Therefore, many countries have adopted bridge management systems (BMSs) to evaluate the conditions of each bridge belonging to the network; in addition, BMSs have proved to be cost-effective tools when it comes to allocate resources and establish management policies (Pellegrino et al., 2011, 2015).

Consequently, the availability of a reliable method to assess the bridge seismic vulnerability is a key factor for the existence of an efficient management system. Different procedures have been developed to investigate the masonry arch bridge response to an earthquake. The first rationally formulated approaches were limit analysis (Castigliano, 1879) and non-linear incremental analysis (Heyman, 1966; Kooharian, 1953), they referred to bi-dimensional arches; improved models took into account the fill (Cavicchi and Gambarotta, 2005), piers (da Porto et al., 2016; Zampieri et al., 2014), soil interaction (Cavicchi and Gambarotta, 2006) and supports' settlement (Zampieri et al., 2018a, b, c). Thanks to the more and more common use of computing machines, three-dimensional FEM models now enable to carry out thorough analyses (Jahangiri et al., 2018; Marefat et al., 2017; Moazam et al., 2017, 2018; Pelà et al., 2009). Notwithstanding the relevant computational development that has taken place recently, traditional and advanced methods have been compared and discussed (Zampieri et al., 2015a, 2015b, 2016). For the time being, the simplified inelastic analysis technique is likely to be the most rational procedure for practical applications, it combines the non-linear static (pushover) analysis and the response spectrum analysis; this method has been introduced in several codes (British Standard (BS), 1998a, b; Federal Emergency Management Agency, 2005).

This work investigates the simplified inelastic analysis technique according to two procedures. The first procedure adopts a deterministic approach and corresponds to a single non-linear static analysis, performed as described in the Eurocodes (British Standard (BS), 1998a, 1998b, 1991a, 1991b,

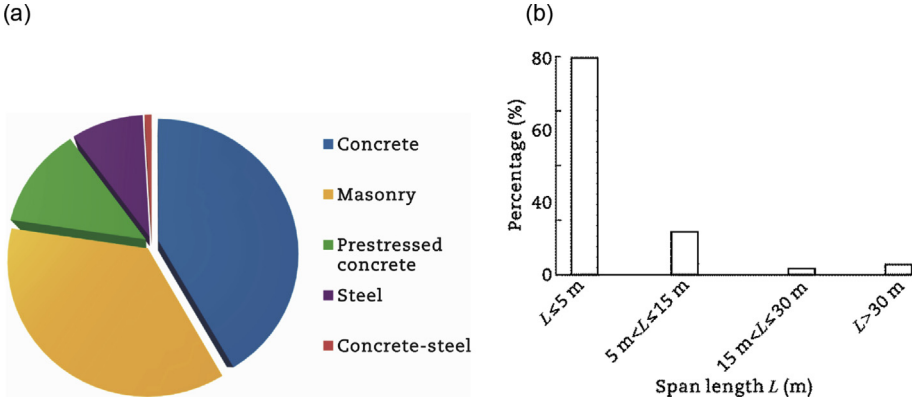

Fig. 1 – Bridges information of Italian railway network. (a) Construction materials. (b) Subdivision of the railway masonry bridges based on their span lengths.

1990, 2010a, 2010b). The second procedures employs a probabilistic approach and considers the variability of the involved mechanical and seismic parameters (Shinozuka et al., 2000a, b). The aim of both the approaches is to evaluate the seismic action the infrastructure can cope with, this can be expressed as a percentage of the ground acceleration defined by the Eurocode national annex (British Standard (BS), 2010b). The goal of this research is to compare these two seismic assessment techniques and their results, as there is currently no code requiring to perform the second analysis procedure.

2. Methodology

2.1. *Bridge survey and investigation campaign*

The research investigates a masonry arch bridge located near Prato municipality along the Florence-Bologna double-track railway line; the structure was built around 1850 (Fig. 2(a),(b)). The bridge has two lowered arch spans: the first span has a length L of 5.0 m, a rise f of 1.2 m (f/L is 0.24) and crosses a brook, the second span has a length L of 3.5 m, a rise f of 0.7 m (f/L is 0.20) and crosses a trafficked road. The bridge has a skew angle of 22° and is 10.3 m wide (Fig. 2(c)).

Bridge geometry, construction details, materials mechanical properties and soil characterization are the four necessary inputs for the creation of structural models (British Standard (BS), 1998b, 2010a). Both destructive and non-destructive testing techniques offer valuable information describing the bridge current condition and provide the key input parameters to conduct structural analyses (Bergamo et al., 2015; Orbán and Gutermann, 2009). The following investigations are performed in reference to the surveyed bridge (Fig. 3).

- Single flat jack. The test estimates the local stress state of the wall. The technique is based on the variation of the stress state at a point in the structure caused by a flat cut

Fig. 3 – Position of the executed tests: single flat jack (single solid line), double flat jack (double solid line), core drilling and boroscopy (dashed line).

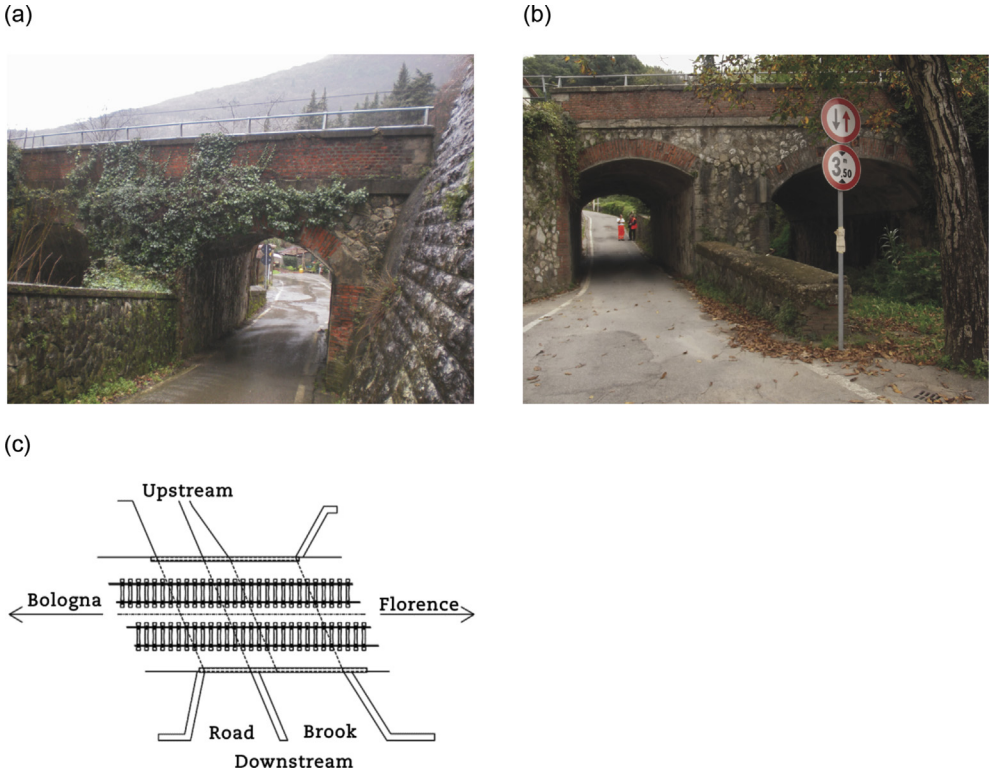

Fig. 2 – Global view of the investigated railway masonry arch bridge. (a) Upstream view. (b) Downstream view. (c) Plan view.

executed in the normal direction to the masonry (ASTM International, 2014a, b).
- Double flat jack. The test estimates compressive strength, longitudinal elasticity modulus and Poisson's ratio of the wall. A double flat cut is executed in the normal direction to the masonry (ASTM International, 2014a, b).
- Mortar characterization. The examination defines the composition, consistency and textural characteristics of the mortar mixture by identification of the aggregates particle size (ASTM International, 2015).
- Core drilling. The inspection characterizes the morphology of the structural elements by investigating thickness and consistency of the internal structure up to a depth of about 2 m.
- Boroscopy. The test comprises direct visual inspection of the cavities in the walls created by core drilling. A small camera is inserted into the drilled borehole and allows a detailed visual study of the construction materials and the possible presence of voids.
- Historical analysis. A rational research based on the available documents and historical drawings gives valuable information about the original construction process.

In addition, the soil geotechnical characterization is necessary to evaluate the local seismic response. The bridge site is located in seismic zone 2 and the maximum horizontal acceleration of the ground is between 0.15*g*-0.20*g* (*g* is gravity acceleration), this range has 10% exceedance probability in 50 years (President of the Ministers Council, 2003). Two soil samples are collected thanks to a 20 m continuous drilling operation and six standard penetration tests (SPTs) are performed using a Raymond sampler (ASTM International, 2011). Furthermore, a multi-channel analysis of surface waves (MASW) assesses the propagation velocity of shear waves $V_{s,30}$ in the first 30 m (Achenbach, 1984; Aki and Richards, 1980).

2.2. Finite element modelling of the surveyed bridge

2.2.1. Geometry

A three-dimensional model is created using MIDAS FEA (MIDAS Information Technology (MIDAS IT), 2009). The model includes all the structural elements that participate in the seismic resistance of the bridge: two arches, pier and abutments; the filling material is treated as a non-structural mass. A fixed constraint is defined 1.50 m below the ground level (both the pier and the abutments extend lower than this depth). The model is placed in a reference system consisting of the axes triad *X* (longitudinal direction), *Y* (transversal direction), *Z* (vertical direction).

2.2.2. Actions on structure

The weight of the ballast and the track corresponds to a uniform layer with a thickness of 0.62 m and density characteristic value equal to 18 kN/m^3 (British Standard (BS), 1991b). The characteristic value of the train traffic per linear meter is 80 kN/m as described by the load model LM71; the train load is spread transversely through the ballast thickness with a 4:1 diffusion ratio (British Standard (BS), 1991a). The train load occupies half span of the first arch (Fig. 4(a)) or of the second arch (Fig. 4(b)) regarding the analyses in longitudinal direction. The train load is uniformly applied throughout the extension of the bridge when it comes to the analyses in transversal direction (Fig. 4(c)).

2.2.3. Constitutive relationships

The numerical analysis of the structure models the masonry as a continuous medium; total strain crack is the non-linear constitutive relationship describing the masonry mechanical behaviour. It is a continuous model (smeared crack model) in which the cracks are assumed distributed in the body, and the total deformation is related to the fracture energy (Lotfi and Benson, 1994, 1991). The constitutive relationship for compressive stresses is linear elastic-perfectly plastic, with f_c being the average compressive strength of the masonry (Fig. 5(a)). The constitutive relationship for tensile stresses is linear elastic with linear softening, the following parameters are defined: average tensile strength of the masonry f_t and tensile fracture energy G_f (Fig. 5(b)).

2.3. Seismic vulnerability assessment of the surveyed bridge

Seismic vulnerability expresses the probability for people, constructions or goods in general to suffer damage due to a seismic phenomenon. This parameter, together with

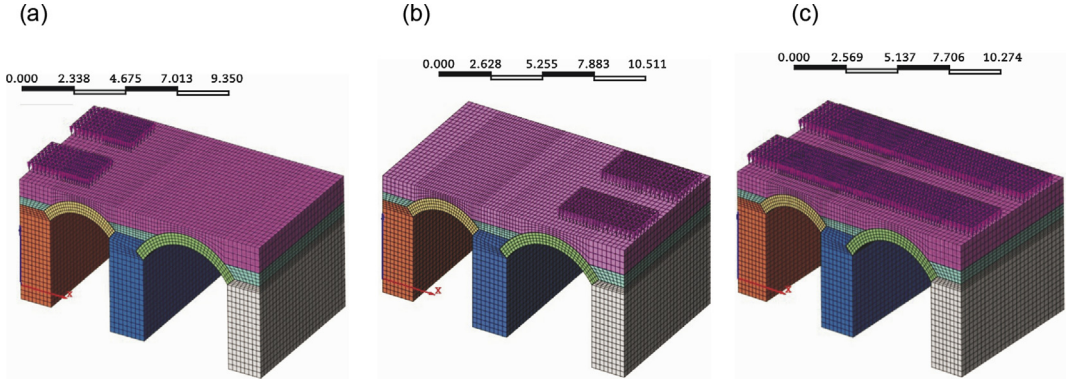

Fig. 4 – Train load application for non-linear static analyses. (a) Earthquake action along in longitudinal direction +X. (b) Earthquake action along longitudinal -X. (c) Earthquake direction along transversal direction ±Y.

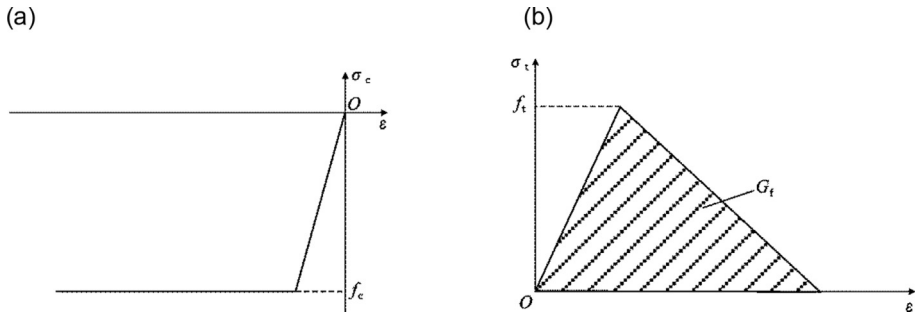

Fig. 5 – Total strain crack model: constitutive relationship. (a) Compression stress. (b) Tensile stress.

exposure and seismic hazard, is related to seismic risk, which is the probability of suffering economic and social losses due to the earthquake associated to a given return period (Cutter, 1996). The goal of seismic vulnerability assessment is to compare the peak ground acceleration (PGA) for the bridge location (seismic demand, PGA_D) with the PGA leading to the bridge collapse (seismic capacity, PGA_C): the risk indicator RI is defined as

$$RI = \frac{PGA_C}{PGA_D} \quad (1)$$

2.4. *Seismic vulnerability assessment: deterministic approach*

2.4.1. *Seismic demand evaluation*

The design working life of the bridge corresponds to category 4, namely 50 years (British Standard (BS), 1990). The importance class is III (British Standard (BS), 1998a) and the corresponding national importance factor γ_I is 1.5 (British Standard (BS), 2010b). The number of years T_L related to the seismic action level, obtained by multiplying the design working life and the importance factor, is 75 (British Standard (BS), 1998a). The seismic action is specified via its return period T_R, which is related to its probability of exceedance P_R in T_L years in accordance with Eq. (2).

$$T_R = -\frac{T_L}{\ln(1-P_R)} \quad (2)$$

Life safety is the target performance level (P_R is equal to 10%) and the associated return period T_R is 712 years (British Standard (BS), 1998a). The reference seismic action is defined by the elastic response spectrum associated to the construction site. The following parameters define the pseudo-acceleration response spectrum $S_e(T)$: ground type, design acceleration a_g on ground type A, ground maximum spectral amplification factor F_0, lower limit of the period of the constant spectral acceleration branch T_B, upper limit of the period of the constant spectral acceleration branch T_C, lower limit of the period of the constant displacement branch T_D, damping factor η, stratigraphic amplification coefficient S_S and topographic amplification coefficient S_T (British Standard (BS), 1998a; British Standard (BS), 2010b). Table 1 reports the parameters values.

Fig. 6 displays the pseudo-acceleration response spectrum $S_e(T)$ as function of the vibration period T of a linear single-degree-of-freedom system; the acceleration $S_e(T)$ is expressed in terms of gravity acceleration g.

The seismic action is combined with the other loads conveniently according to the expression

$$\sum_{j\geq 1} G_{k,j} + A_{Ed} + \sum_{i\geq 1} \psi_{2i} Q_{k,i} \quad (3)$$

where $G_{k,j}$ is the characteristic value of the jth permanent action, A_{Ed} is the design value of seismic action, $Q_{k,i}$ is the value of the ith variable action and $\psi_{2i}\, Q_{k,i}$ is the quasi-permanent value of the ith variable action (British Standard (BS), 1991a, 1991b, 1990).

2.4.2. *Non-linear static analysis*

Non-linear static analysis, also known as pushover analysis, is the method used to evaluate the global seismic response of the surveyed bridge. The analysis includes the determination of a force–displacement relationship (capacity curve), which is usually represented by displaying the displacement of a chosen control point of the structure along the x-axis and the total applied shear force along the y-axis. The maximum displacement of the structure is evaluated by the seismic action defined by the response spectrum (British Standard (BS), 1998a). The mechanical parameters of the structures are the ones obtained from the bridge survey. The non-linear static analysis of the masonry bridge is carried out considering both longitudinal and transverse directions.

2.5. *Seismic vulnerability assessment: probabilistic approach*

The analytical determination of the fragility function is a useful approach to evaluate the seismic vulnerability of a structure (Zampieri et al., 2016). A fragility curve defines the conditional probability of exceeding a specified level of

Table 1 – Parameters defining the pseudo-acceleration response spectrum.

Parameter	a_g (g)	F_0	T_B (s)	T_C (s)	T_D (s)	η	S_S	S_T
Value	0.196	2.390	0.138	0.413	2.383	1	1.20	1.20

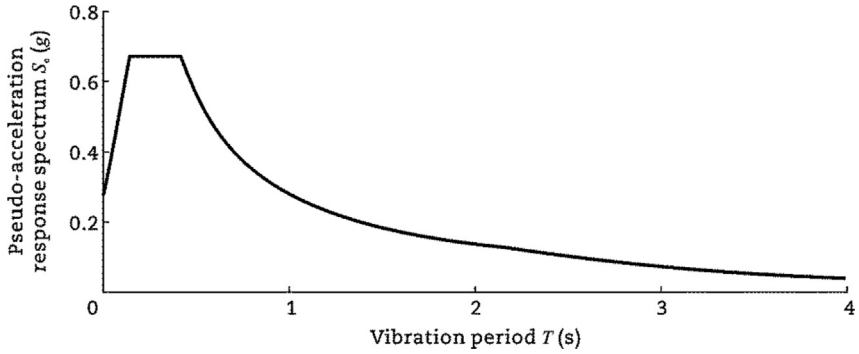

Fig. 6 – Pseudo-acceleration response spectrum.

damage associated to an intensity level of the seismic action. The curve is represented in a graph plotting the intensity of the earthquake (PGA) along the *x*-axis and the probability of exceeding the damage level to which the curve refers along the *y*-axis. The determination of the fragility function comprises three main steps:

- simulation of the bridge taking into account the uncertainties related to its structural properties, – simulation of the seismic action based on recorded or generated earthquakes, – generation of fragility curve based on the response data obtained from the numerical model.

Fragility curves allow to take into consideration the uncertainty of the various components involved in the definition of the seismic vulnerability from a probabilistic point of view. This is valid for both the seismic capacity (structure geometry and mechanical properties of the building materials) and the seismic demand (intensity of the action and site conditions); their variations can be described by using probabilistic distributions. The intersection between the capacity curve and the demand curve is called performance point; therefore, the performance point of the structure is no longer represented by an exact value as in the deterministic analysis, but by a set of values. Fig. 7 shows this concept in the acceleration-displacement response spectrum (ADRS) plane. The capacity spectrum method (CSM) is the approach used for the construction of the fragility curve (Shinozuka et al., 2000a, b).

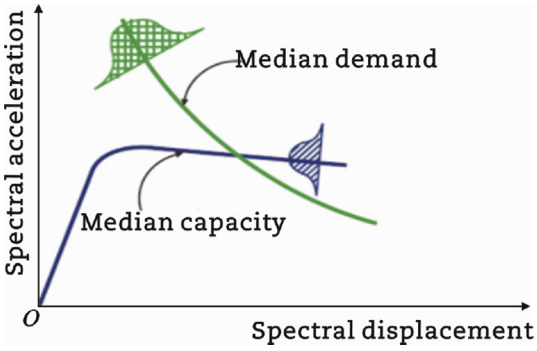

Fig. 7 – Uncertainties related to capacity and demand curves in the ADRS plane (Mander and Basoz, 1999).

2.5.1. Probability distribution of the materials mechanical properties

In order to perform the vulnerability seismic assessment of the masonry arch bridge adopting a probabilistic approach, a sufficient large database describing the mechanical properties of this type of structure is necessary. 107 railway masonry arch bridges are investigated by means of a single and double flat jack. Italian railway network has an internal instruction referred to as 44C (Italian Railway Network, 2014) based on UIC guidelines (Union Internationale des Chemins de fer (UIC), 2009b); the goal of Instruction 44C is to provide a sound methodology to assess the conservation state of railway infrastructures through technical surveys taking place with a specified frequency. This procedure considers different defects or distresses affecting the structure (i.e., moisture spots, efflorescence and material exfoliation), their surface extension and intensity. Afterwards, each surveyed structure is given a number expressing its conservation state. Even if the 107 considered bridges are distributed across the country and their environmental conditions are not necessarily the same, they approximately have the same age; moreover the current preservation conditions, showing defects and distresses, are similar. Two mechanical parameters are of particular interest, namely masonry compressive strength $f_{c,mean}$ and longitudinal elasticity modulus E_{mean}.

In addition, the outcomes of this extensive investigations are compared to the corresponding values: mean compressive strength $f_{c,code}$ and mean longitudinal elasticity modulus E_{code} of masonry defined by the Eurocode national annex (British Standard (BS), 2010a). This code lists 11 different types of masonry walls. The quantity of the experimental data is sufficient to make a comparison regarding the following categories: type 2 (rough-hewn rubble wall, with a limited thickness and internal core), type 3 (hewn rubble wall, with good texture) and type 6 (solid brick wall and lime mortar). For each type of masonry wall, the occurrence of the experimental values is initially divided into adequate intervals (Fig. 8(a)), the lognormal probabilistic distribution describes the data dispersion (Fig. 8(b)), finally, the mean value associated to the investigations and the ones provided by the code are compared (Fig. 8(c)); for example, Fig. 8 shows this operation for the compressive strength parameter f_c. Since some structures may show particularly good or poor preservation conditions, the use of a big set

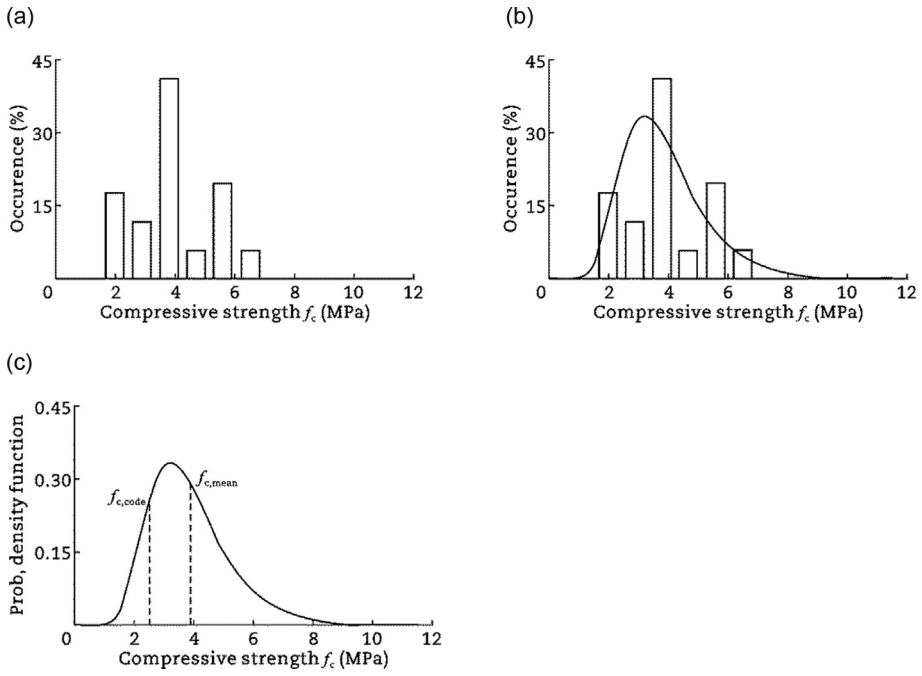

Fig. 8 – Compressive strength parameter. (a) Subdivision of experimental values. (b) Lognormal probabilistic distribution. (c) Mean values comparison.

(107) of bridges is a necessary input; therefore, the statistical data treatment is a desirable approach.

The probabilistic distributions of masonry compressive strength f_c and longitudinal elasticity modulus E are the relevant mechanical parameters MP: the structural analyses take into consideration their probabilistic distribution. The probability density functions of f_c and E are adequately discretized in three parts. The arches of the surveyed bridge correspond to masonry type 6, the pier and the abutments to type 2.

2.5.2. *Probability distribution of the seismic demand*

To build a robust fragility function, it is important to consider a sufficiently large set of ground motions to cover the PGA intensity range of interest (Negulescu et al., 2014); both recorded or simulated accelerograms can be used (Choi et al., 2004). Ground acceleration registrations are selected from the Italian accelerometric archive (ITACA) according to the following criteria: signals recorded on ground type A or B, local magnitude between 5.5 and 6.5 and epicentral distance up to 30 km (Luzi et al., 2017), the choice of these parameters' values guarantees the availability of seismic data in sufficient quantity. 75 registered accelerograms are selected and the relative elastic spectra are calculated with damping ξ equal to 0.05. These accelerograms are grouped in 5 intervals based on their maximum PGA (0.50–1.50, 1.50–2.50, 2.50–3.50, 3.50–4.50, 4.50–5.50 m/s^2), each group includes 15 registrations. The following spectra are evaluated for each PGA interval: average spectrum, average spectrum plus the positive standard deviation σ^+ and the average spectrum minus the negative standard deviation σ^-; therefore, 15 seismic inputs M are considered.

For instance, Fig. 9 illustrates this procedure regarding the PGA range 0.50–1.50 m/s^2. Fig. 9(a),(b) shows the acceleration and displacement mean response spectra (MRS) of 15 time histories, respectively. Fig. 9(c),(d) displays the MRS in acceleration and in displacement, respectively, including the standard deviations. Fig. 9(e) reports the MRS and the standard deviations in the ADRS plane.

2.5.3. *Fragility curve calculation*

Each PGA range comprises 3 spectra: mean spectrum, mean spectrum plus positive standard deviation σ^+ and mean spectrum minus negative standard deviation σ^-; since 5 PGA ranges are considered, the total amount of seismic inputs M considered is 15. For the ith PGA range interval, there are three spectra: $ADRS_i$, $ADRS_{i^+\sigma^+}$, $ADRS_{i^-\sigma^-}$. Considering the jth bridge characterized by the jth combination of mechanical parameters MP_j (namely $f_{c,mean,j}$ and $E_{mean,j}$), three intersection values (performance points) are identified: d^*_{max} ($ADRS_i$, MP_j), d^*_{max} ($ADRS_{i^+\sigma^+}$, MP_j) and d^*_{max} ($ADRS_{i^-\sigma^-}$, MP_j), Fig. 10.

On a general basis, the values of the positive standard deviation σ_i^+ and the negative standard deviation σ_i^- do not coincide; therefore, the average displacement value d^*_{max} ($ADRS_i$) and the standard deviation $\sigma_i = (\sigma_i^+\sigma_i^-)^{1/2}$ are evaluated.

Considering that the probability density functions of the mechanical parameters MP are discretized in three parts and that two types of masonry walls compose the surveyed bridge, there are $3^4 = 81$ combinations involving MP. Consequently, the total amount of structural inputs N considered is equal to 81, each sample bridge is characterized by a jth combination of the mechanical parameters MP_j.

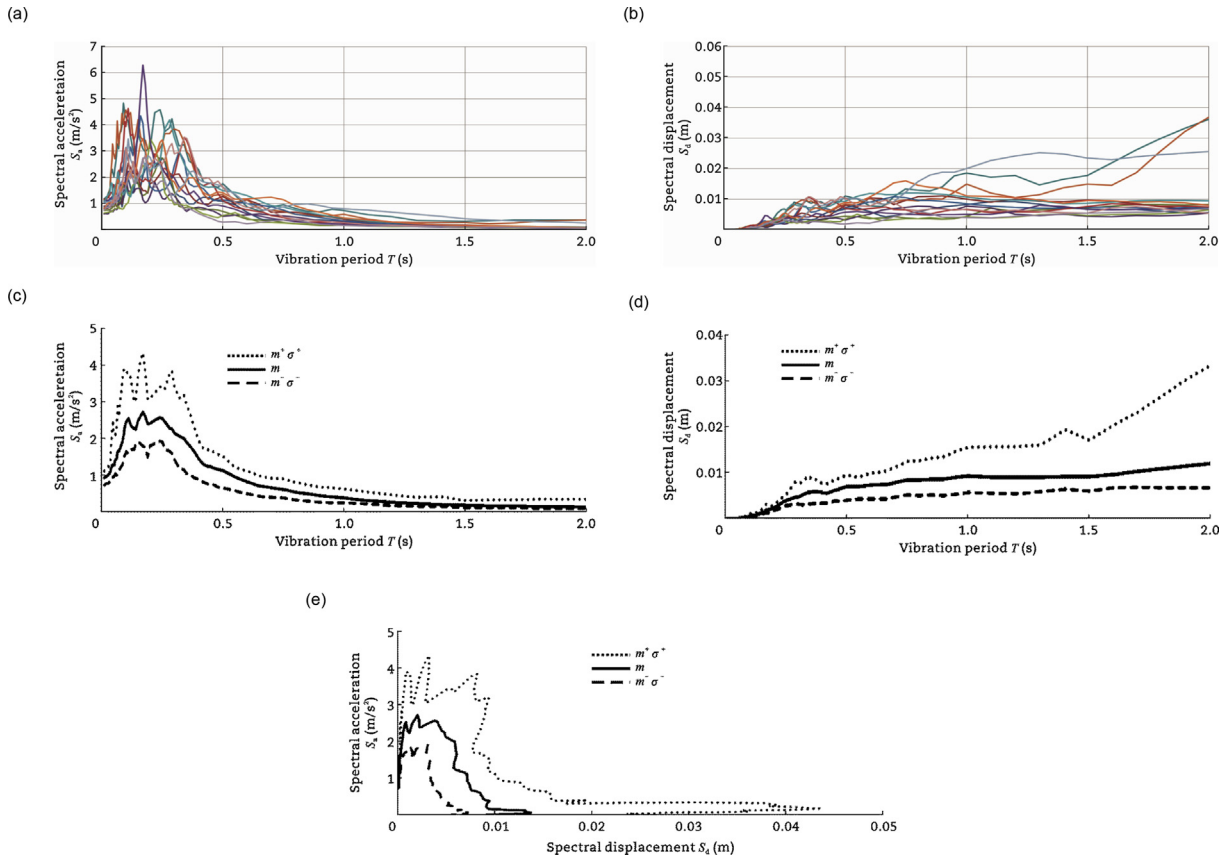

Fig. 9 – Selection of seismic data input for PGA range 0.50–1.50 m/s^2. (a) Acceleration MRS of 15 histories. (b) Displacement MRS of 15 histories. (c) Acceleration MRS and standard deviations from the considered histories. (d) Displacement MRS and standard deviations from the considered histories. (e) MRS and standard deviations in ADRS plane from the considered histories.

The lognormal distribution related to the damage of the jth bridge is obtained by

$$d^*_{\max}(\mathrm{PGA},\mathrm{MP}_j) = c(\mathrm{PGA},\mathrm{MP}_j)\, e^{\frac{\zeta^2(\mathrm{PGA},\mathrm{MP}_j)}{2}} \tag{4}$$

$$\sigma^2(\mathrm{PGA},\mathrm{MP}_j) = \left[d^*_{\max}(\mathrm{PGA},\mathrm{MP}_j)\right]^2 \left[e^{\zeta^2(\mathrm{PGA},\mathrm{MP}_j)} - 1\right] \tag{5}$$

where the two parameters $\zeta(\mathrm{PGA},\mathrm{MP}_j)$, $c(\mathrm{PGA},\mathrm{MP}_j)$ are derived. The probability of exceeding the specified damage level d_1 is assessed as

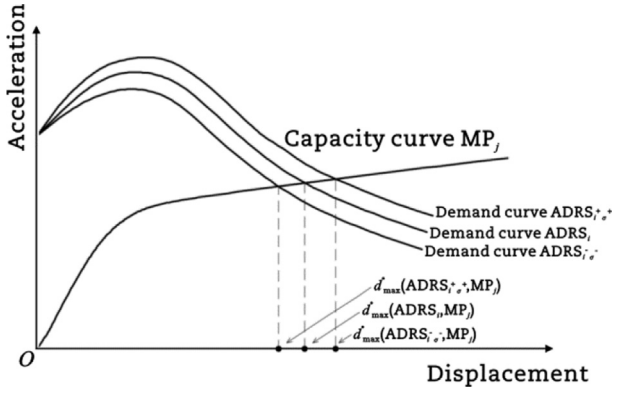

Fig. 10 – Performance points evaluation for jth structure capacity curve and ith seismic demand curve.

$$P_j\left[d^*_{\max}(\mathrm{PGA},\mathrm{MP}_j) > d_{1,j}\right] = 1 - \Phi\left[\frac{\ln\left(\frac{d_{1,j}}{c(\mathrm{PGA},\mathrm{MP}_j)}\right)}{\zeta(\mathrm{PGA},\mathrm{MP}_j)}\right] \tag{6}$$

where Φ is the standardized normal distribution function. The fragility value is obtained as the arithmetic average (Eq. (7))

$$F(\mathrm{PGA}, d_1) = \frac{\sum_{j=1}^{N} P_j(\mathrm{PGA}, d_{1,j})}{N} \tag{7}$$

where N is the total amount of structural inputs considered.

3. Results and discussion

3.1. *Bridge state of conservation*

The results derived from the survey procedures described in section 2.1 are presented below. Tables 2 and 3 display the

Table 2 – Single flat jack investigation: vertical stress state.

Bridge part	Vertical stress (MPa)
Across road	0.08
Across brook	0.12

Table 3 – Double flat jack investigation: vertical stress state, compressive strength, longitudinal elasticity modulus and Poisson's ratio.

Bridge part	Vertical stress (MPa)	Compressive strength (MPa)	Longitudinal elasticity modulus (MPa)	Poisson's ratio
Across road	0.12	2.01	3323	0.22
Across brook	0.12	4.03	2052	0.19

Table 4 – Mortar characterization for the bridge part crossing the road.

Texture	Component	Mass (%)
Matrix	Carbonatic structure	25
Binder	Irregular shape	20
Aggregates	Quartz (44%)	55
	Limestone (25%)	
	Plagioclase (15%)	
	Metamorphic minerals (6%)	
	Sandstone (5%)	
	Igneous minerals (5%)	

Table 5 – Mortar characterization for the bridge part crossing the brook.

Texture	Component	Mass (%)
Matrix	Carbonatic structure	32
Binder	Irregular shape	8
Aggregates	Quartz (30%)	60
	Plagioclase (30%)	
	Metamorphic minerals (25%)	
	Sandstone (15%)	

outcomes of single and double flat jack investigations, respectively.

The mortar of the bridge part crossing the road contains silica calcareous sand, Table 4 describes its components. The mortar of the bridge part crossing the brook is brown with prevailing feldspar sand, Table 5 describes its components.

Thin-section microscopy images of mortar samples show mineralogy and grain size, Fig. 11. Core drilling and boroscopy are carried out as depicted in Fig. 12.

No fractures or discontinuities are found with the boroscopy surveys; the bricks bounded with mortar are in good condition. Furthermore, the thickness of the material layers composing the arches match well with the geometrical dimensions reported in the historical drawings.

3.2. *Mechanical parameters of the surveyed bridge*

Based on the acquired information about geometry, construction details and properties of the building materials, the knowledge level is KL2 (normal) and the corresponding confidence factor CF_{KL2} is equal to 1.20 (British Standard (BS), 1998b). The parameters determined for the masonry are: average compressive strength f_m, average shear strength τ_0, average normal elasticity modulus E, average tangential elasticity modulus G and average specific weight w (British Standard (BS), 2010a).

The masonry of the arches is type 6 (solid brick wall and lime mortar), the masonry of the pier and the abutments is type 2 (rough-hewn rubble wall, with a limited thickness and internal core); Table 6 displays the design parameters. The density value associated to the filling material is 20 kN/m^3.

The parameter $V_{s,30}$ of the ground is 385 m/s, which corresponds to ground type B (British Standard (BS), 1998b).

3.3. *Seismic vulnerability assessment result: deterministic approach*

Considering the results of the previous section 3.2, Table 7 display the parameters used to define the total strain crack model (described in subsection 2.2.3).

Two load profiles applications are considered, both in the longitudinal and transversal direction: one profile is proportional to the masses and the other is proportional to the vibrating modes (British Standard (BS), 1998a). The most severe condition is associated to the first vibration mode, which is predominantly longitudinal; its vibration period is 0.18 s and is characterized by 63% participating mass (Fig. 13).

The control node used to determine the capacity curves both in longitudinal and transversal direction is located at the central top of the pier. Fig. 14(a) displays the capacity curve associated to the longitudinal analysis with load profile proportional to the first mode vibration; Fig. 14(b) represents the cracking state corresponding to the end of the capacity

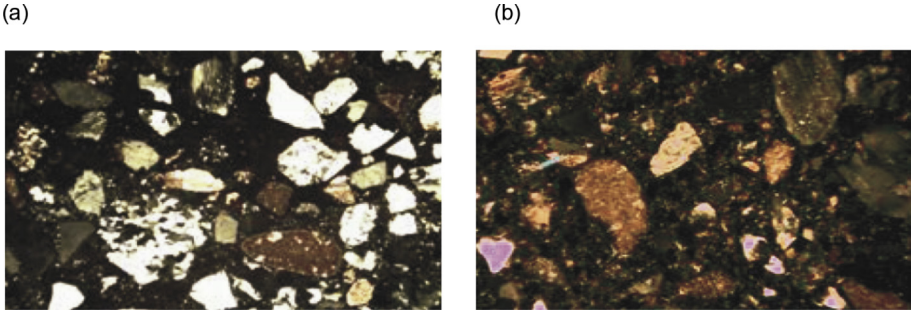

Fig. 11 – Mortar mineralogy and grain size for the bridge part (optical micrographs, transmitted plane-polarized light, 20x). (a) Crossing the road. (b) Crossing the brook.

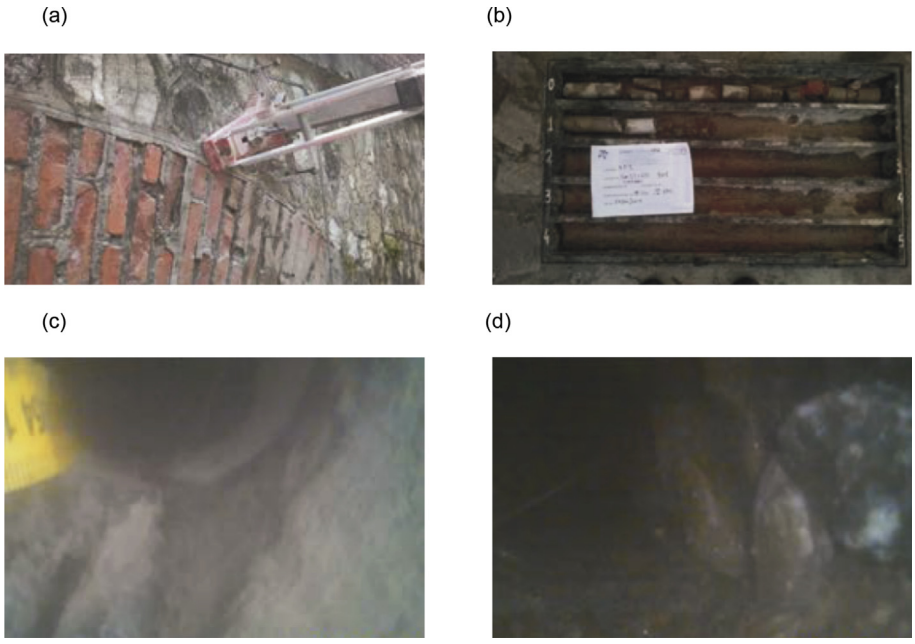

Fig. 12 – Drilling and boroscopy procedure for each investigated location. (a) Core drilling. (b) Cored samples. (c) Visual inspection inside the core. (d) Visual inspection at the core end.

Table 6 – Design parameters of the masonry constituting the arch bridge.

Element	f_m (MPa)	τ_0 (MPa)	E (MPa)	G (MPa)	w (kN/m^3)
Arch	4.00	0.095	2250	750	18
Pier, abutments	2.08	0.036	1230	410	20

Table 7 – Parameters for the total strain crack model.

Element	f_t (N/mm^2)	G_f (N/mm)	f_c (N/mm^2)
Arch	0.200	0.01	4.000
Pier, abutments	0.104	0.01	2.083

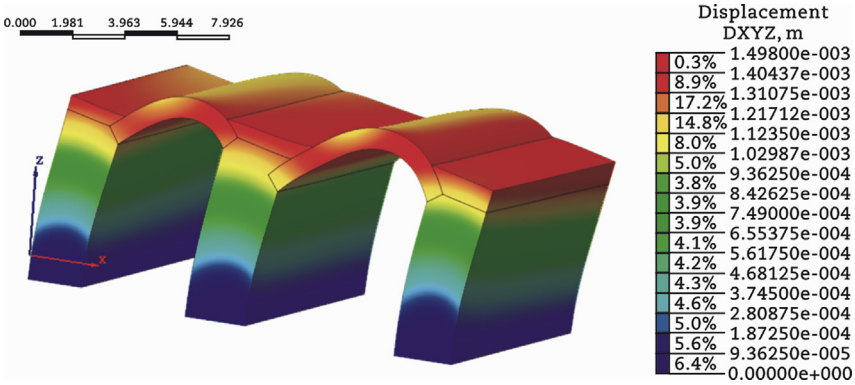

Fig. 13 – First mode vibration form of the surveyed bridge.

curve, the general failure of the bridge is assumed in this condition.

The seismic demand PGA_D is 0.282*g* and the seismic capacity of the structure PGA_C is 0.160*g*, the corresponding risk indicator RI is 0.57.

3.4. *Seismic vulnerability assessment result: probabilistic approach*

3.4.1. *Mechanical parameters of the 107 railway network bridges*

Figs. 15–17 display the following content for each investigated type of masonry wall: an image of the masonry category, the comparison between experimental mean value of the compressive strength $f_{c,mean}$ and the corresponding value from code $f_{c,code}$ and the comparison between the experimental mean value of longitudinal elasticity modulus E_{mean} and the corresponding value from code E_{code}. Fig. 15 is associated to masonry type 2 (rough-hewn rubble wall, with a limited thickness and internal core), Fig. 16 to type 3 (hewn rubble wall, with good texture) and Fig. 17 to type 6 (solid brick wall and lime mortar).

Table 8 summarizes the results and the differences regarding the masonry compressive strength; similarly, Table 9 summarizes the results and the differences regarding the masonry longitudinal elasticity modulus.

As specified in subsection 2.5.1, the probability density functions associated to the mechanical parameters f_c and E are discretized in three intervals. Fig. 18 refers to masonry type 6, which composes the arches of the bridge; Fig. 19 refers to masonry type 2, which composes the pier and the abutments.

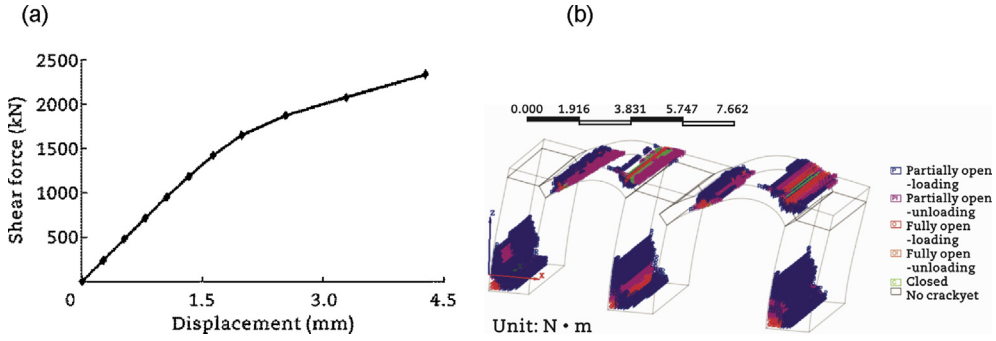

Fig. 14 – Deterministic analysis result. (a) Capacity curve of the surveyed bridge. (b) Plasticized areas at the end of the capacity curve.

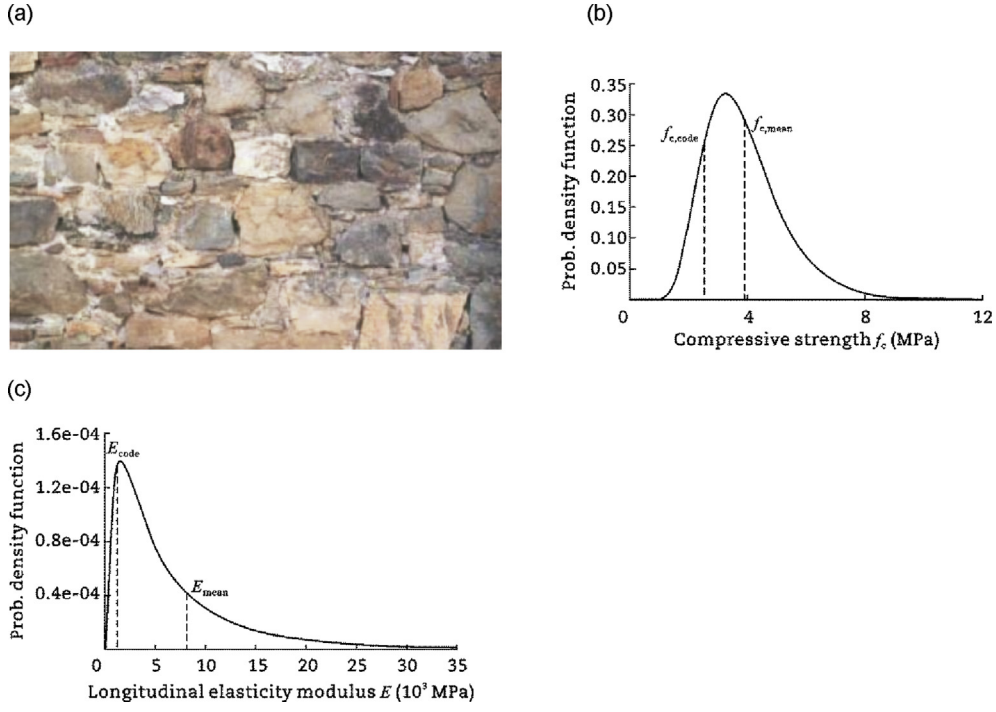

Fig. 15 – Masonry wall type 2. (a) Photograph. (b) Comparison between experimental and code values of compressive strength. (c) Comparison between experimental and code values of longitudinal elasticity modulus.

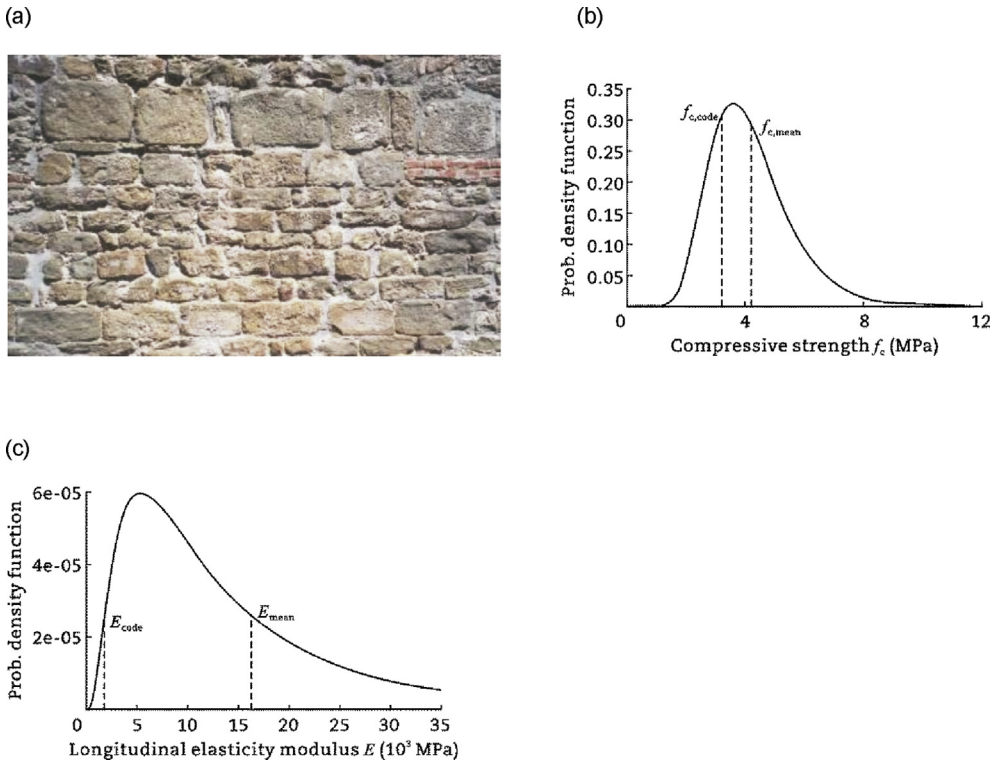

Fig. 16 – Masonry wall type 3. (a) Photograph. (b) Comparison between experimental and code values of compressive strength. (c) Comparison between experimental and code values of longitudinal elasticity modulus.

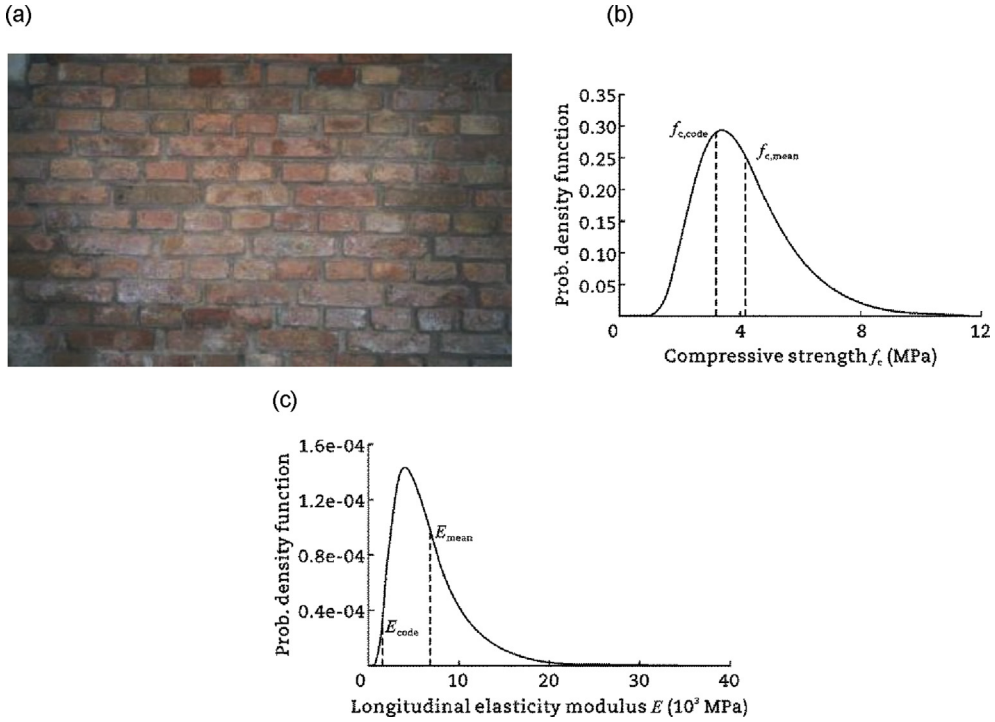

Fig. 17 – Masonry wall type 6. (a) Photograph. (b) Comparison between experimental and code values of compressive strength. (c) Comparison between experimental and code values of longitudinal elasticity modulus.

Table 8 – Comparison between experimental and code values of compressive strength for different masonry wall types.

	$f_{c,mean}$ (MPa)	$f_{c,code}$ (MPa)	$(f_{c,mean} - f_{c,code})/f_{c,code}$ (%)
Masonry wall type 2	3.87	2.50	54.9
Masonry wall type 3	4.20	3.20	31.3
Masonry wall type 6	4.17	3.20	30.3

Table 9 – Comparison between experimental and code values of longitudinal elasticity modulus for different masonry wall types.

	E_{mean} (MPa)	E_{code} (MPa)	$(E_{mean} - E_{code})/E_{code}$ (%)
Masonry wall type 2	8146	1230	562
Masonry wall type 3	16,199	1740	831
Masonry wall type 6	6717	1500	348

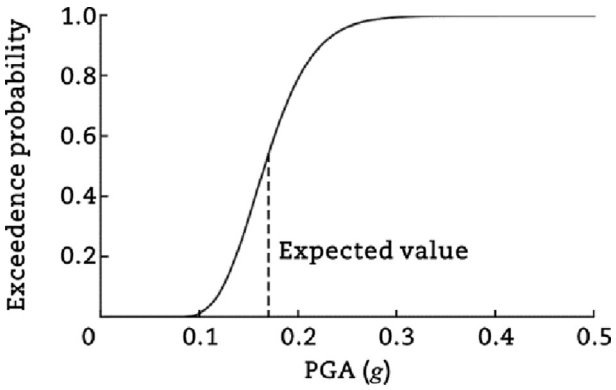

Fig. 20 – Fragility curve of the surveyed bridge for life safety performance level.

3.4.2. *Fragility curve generation*

A total of *N* models are created with MIDAS FEA and *N* capacity curves are extracted; these analyses are performed along the longitudinal distribution in line with the deterministic approach. The fragility curve obtained for the surveyed bridge referring to the considered life safety performance level is shown in Fig. 20. The seismic capacity PGA_C is 0.165*g*, therefore the index risk IR is 0.59.

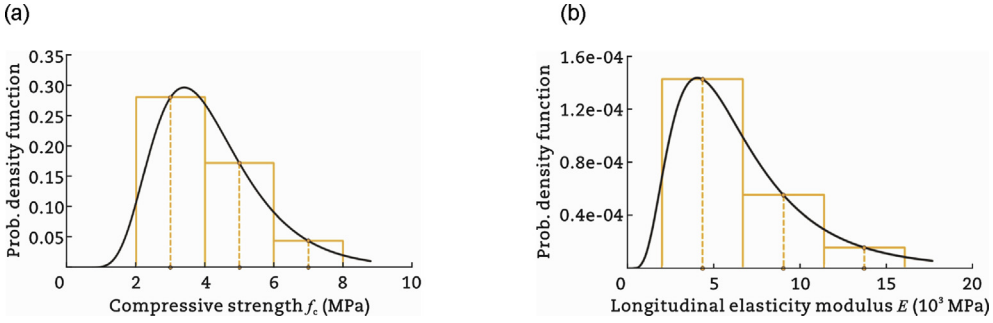

Fig. 18 – Discretization of probability density function for masonry type 6. (a) Compressive strength. (b) Longitudinal elasticity modulus.

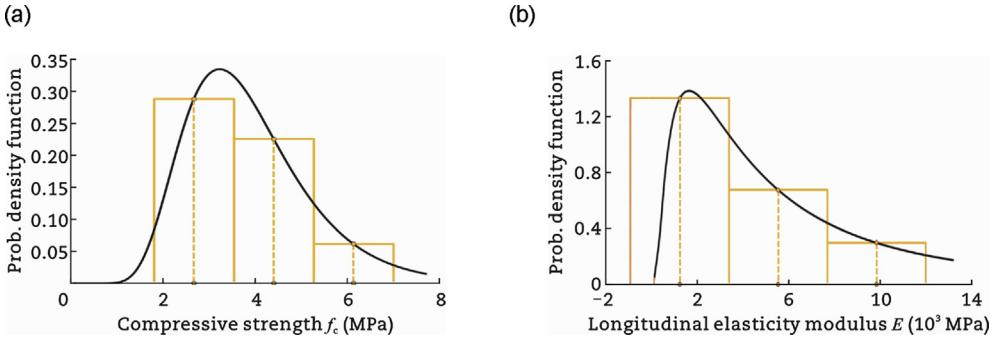

Fig. 19 – Discretization of probability density function for masonry type 2. (a) Compressive strength. (b) Longitudinal elasticity modulus.

4. Conclusions

This work dealt with the seismic vulnerability assessment of a railway masonry arch bridge located near Prato municipality along the Florence-Bologna double-track railway line. An extensive in-situ investigation gathered the necessary information about the structural mechanical parameters of the bridge. Two methods were used to assess its seismic vulnerability. One approach was the non-linear static analysis performed from a deterministic point of view: only the data obtained from the in-situ investigation were used. The second approach adopted a probabilistic point of view. In order to carry out this analysis, knowledge about the variability of both the seismic inputs and the material structural inputs was necessary. Particular registered accelerograms described the seismic demand. The results from an extensive in-situ investigation comprising 107 railway masonry arch bridges described the structural parameters. In addition, this survey enabled a comparison between the experimental values and the values specified by the Eurocode. The following considerations may be drawn.

(1) Both the deterministic and probabilistic approaches highlight that the risk index is smaller than the unity; as a consequence of this, retrofitting operations are necessary for the bridge to reach an acceptable safety condition.
(2) The risk indexes obtained with the deterministic and probabilistic approaches are similar. Nevertheless, the fragility curve allows to take into account the probability of overcoming the PGA, to deal with various damage levels and, above all, to evaluate the effect of the considerable variability of the seismic input.
(3) The calculation of the fragility curves represents an effective tool for the description of seismic damage scenarios. This has an important role when it comes to establishing the priority order of assets intervention.
(4) All the values of masonry compressive strength and longitudinal elasticity modulus proposed by the Eurocode underestimate the experimental findings. Therefore, the railway authority could establish its own reference values, this would bring to a better asset management and improved business policies.

Conflict of interest

The author does not have any conflict of interest with other entities or researchers.

Acknowledgments

This work was supported by a collaboration between Sapienza University of Rome and Standard Infrastructure Civil and Experimental, Italian Railway Network (RFI).

List of symbols

A_{Ed}	Design value of seismic action
c(PGA, MP)	Parameter for fragility curve determination
d^*_{max}	Displacement value, performance point
d_l	Damage level for fragility curve determination
E	Masonry longitudinal elasticity modulus
E_{code}	Masonry longitudinal elasticity modulus from Eurocode national annex
E_{mean}	Masonry average longitudinal elasticity modulus
F(PGA, d_l)	Fragility curve value
F_0	Ground maximum spectral amplification factor
f	Arch span rise
f_c	Masonry compressive strength
$f_{c,code}$	Masonry average compressive strength from Eurocode national annex
$f_{c,mean}$	Masonry average compressive strength
f_m	Masonry average compressive strength for existing structure
f_t	Masonry average tensile strength
G	Masonry tangential elasticity modulus
G_f	Masonry tensile fracture energy
$G_{k,j}$	Characteristic value of the j-th permanent action
g	Gravity acceleration (9.81 m/s^2)
L	Arch span length
P_R	Exceedance probability
$Q_{k,i}$	Value of the ith variable action
$S_e(T)$	Pseudo-acceleration response spectrum
S_S	Stratigraphic amplification coefficient
S_T	Topographic amplification coefficient
T_B	Lower limit of the period of the constant spectral acceleration branch
T_C	Upper limit of the period of the constant spectral acceleration branch
T_D	Lower limit of the period of the constant displacement branch
T_L	Number of years related to the seismic action level
T_R	Return period
$V_{s,30}$	Shear vawes propagation velocity in the first 30 m from surface level
w	Masonry average specific weight for existing structure
γ_I	Importance factor from Eurocode national annex
ζ(PGA, MP)	Parameter for fragility curve determination
η	Generalized damping factor, $\eta = [10/(5+\xi)]^{0.5}$
ξ	Conventional damping factor (0.05)
σ^+	Positive standard deviation
σ^-	Negative standard deviation
T_0	Masonry average shear strength for existing structure
Φ	Standardized normal distribution function
$\psi_{2i}\, Q_{k,i}$	Quasi-permanent value of the ith variable action

List of abbreviations

ADRS	Acceleration-displacement response spectrum
BMS	Bridge management system
CF	Confidence factor

CSM	Capacity spectrum method
KL	Knowledge level
MASW	Multi-channel analysis of surface waves
MP	Mechanical parameters
MRS	Mean response spectra
PGA	Peak ground acceleration
PGA_C	Peak ground acceleration, seismic capacity
PGA_D	Peak ground acceleration, seismic demand
RI	Risk Indicator
SPT	Standard penetration test

REFERENCES

Achenbach, J., 1984. Wave Propagation in Elastic Solids, vol. 16. North Holland, Amsterdam.

Aki, K., Richards, P., 1980. Quantitative Seismology, first ed. W.H. Freeman & Co Ltd, New York.

ASTM International, 2011. Standard Test Method for Standard Penetration Test (SPT) and Split-barrel Sampling of Soils. ASTM, West Conshohocken.

ASTM International, 2014a. Standard Test Method for in Situ Measurement of Masonry Deformability Properties Using the Flatjack Method. ASTM, West Conshohocken.

ASTM International, 2014b. Standard Test Method for in Situ Compressive Stress within Solid Unit Masonry. ASTM, West Conshohocken.

ASTM International, 2015. Standard Test Method for Examination and Analysis of Hardened Masonry Mortar. ASTM, West Conshohocken.

Bergamo, O., Campione, G., Donadello, S., et al., 2015. In-situ NDT testing procedure as an integral part of failure analysis of historical masonry arch bridges. Engineering Failure Analysis 57, 31–55.

British Standard (BS), 1990. Eurocode Basis of Structural Design. BSI Group, London.

British Standard (BS), 1991a. Eurocode 1 Basis of Design and Action on Structures – Part 2 Traffic Loads on Bridges. BSI Group, London.

British Standard (BS), 1991b. Eurocode 1 Basis of Design and Action on Structures – Part 1.1 Actions on Structures-densities, Self-weight and Imposed Loads. BSI Group, London.

British Standard (BS), 1998a. Eurocode 8 Design of Structures for Earthquake Resistance – Part 1 General Rules, Seismic Actions and Rules for Buildings. BSI Group, London.

British Standard (BS), 1998b. Eurocode 8 Design of Structures for Earthquake Resistance – Part 3: Assessment and Retrofitting of Buildings. BSI Group, London.

British Standard (BS), 2010a. Eurocode 8 Design of Structures for Earthquake Resistance – Part 3 Assessment and Retrofitting of Buildings. BSI Group, London.

British Standard (BS), 2010b. Eurocode 8 Design of Structures for Earthquake Resistance – Part 1 General Rules, Seismic Actions and Rules for Buildings. BSI Group, London.

Castigliano, A., 1879. Theorie de l'equilibre des systemes elastiques et ses applications. Negro, Augusto Federico, Turin.

Cavicchi, A., Gambarotta, L., 2005. Collapse analysis of masonry bridges taking into account arch–fill interaction. Engineering Structures 27, 605–615.

Cavicchi, A., Gambarotta, L., 2006. Two-dimensional finite element upper bound limit analysis of masonry bridges. Computers and Structures 84 (31–32), 2316–2328.

Choi, E., DesRoches, R., Nielson, B., 2004. Seismic fragility of typical bridges in moderate seismic zones. Engineering Structures 26 (2), 187–199.

Cocciaglia, D., Mosca, L., 1998. Bearing Capacity of RailCway Arch Bridges. La Tecnica Professionale. Rete Ferroviaria Italiana, Rome.

Cutter, S.L., 1996. Vulnerability to environmental hazards. Progress in Human Geography 20 (4), 529–539.

da Porto, F., Tecchio, G., Zampieri, P., et al., 2016. Simplified seismic assessment of railway masonry arch bridges by limit analysis. Structure and Infrastructure Engineering 12 (5), 567–591.

Federal Emergency Management Agency, 2005. FEMA 440: Improvement of Nonlinear Static Seismic Analysis Procedures. Federal Emergency Management Agency, Washington DC.

Heyman, J., 1966. The stone skeleton. International Journal of Solids and Structures 2 (2), 249–279.

Italian Railway Network, 1907. Modalità par la compilazione dei progetti dei manufatti. Rete Ferroviaria Italiana, Rome.

Italian Railway Network, 2014. Instruction 44C Inspections of Bridges, Tunnels and Other Railway Infrastructures. Rete Ferroviaria Italiana, Rome.

Jahangiri, V., Yazdani, M., Marefat, M.S., 2018. Intensity measures for the seismic response assessment of plain concrete arch bridges. Bulletin of Earthquake Engineering 16 (9), 4225–4248.

Kooharian, A., 1953. Limit analysis of voussoir (segmental) and concrete arches. International Concrete Abstracts Portal 49 (12), 317–328.

Lotfi, H., Benson, S., 1994. Interface model applied to fracture of masonry structures. Journal of Structural Engineering 120 (1), 63–80.

Lotfi, H., Benson, S., 1991. An appraisal of smeared crack models for masonry shear wall analysis. Computers and Structures 41 (3), 413–425.

Luzi, L., Pacor, F., Puglia, R., 2017. Italian Accelerometric Archive v2.3. Available at: https://doi.org/10.13127/ITACA.2.3. (Accessed 3 September 2018).

Mander, J., Basoz, N., 1999. Fragility curve development for assessing the seismic vulnerability of highway bridges. In: 5th US Conference on Lifeline Earthquake Engineering, Seattle, 1999.

Marefat, M.S., Yazdani, M., Jafari, M., 2017. Seismic assessment of small to medium spans plain concrete arch bridges. European Journal of Environmental and Civil Engineering, https://doi.org/10.1080/19648189.2017.1320589.

MIDAS Information Technology (MIDAS IT), 2009. MIDAS FEA v2.9.6 Nonlinear and Detail FE Analysis System for Civil Structures. MIDAS IT, Seoul.

Moazam, A.M., Hasani, N., Yazdani, M., 2018. Three-dimensional modelling for seismic assessment of plain concrete arch bridges. Proceedings of the Insitution of Civil Engineers Civil Engineering 171 (3), 135–143.

Moazam, A.M., Hasani, N., Yazdani, M., 2017. 3D simulation of railway bridges for estimating fundamental frequency using geometrical and mechanical properties. Advances in Compututional Design 2, 257–271.

Modena, C., Tecchio, G., Pellegrino, C., et al., 2015. Reinforced concrete and masonry arch bridges in seismic areas: typical deficiencies and retrofitting strategies. Structure and Infrastructure Engineering 11 (4), 415–442.

Negulescu, C., Ulrich, T., Baills, A., et al., 2014. Fragility curves for masonry structures submitted to permanent ground displacements and earthquakes. Natural Hazards 74 (3), 1461–1474.

Orbán, Z., Gutermann, M., 2009. Assessment of masonry arch railway bridges using non-destructive in-situ testing methods. Engineering Structures 31 (10), 2287–2298.

Paulsson, B., Olofsson, J., Elfgren, L., et al., 2008. Sustainable bridges – assessment for future traffic demands and longer lives for railway bridges. In: 8th World Congress on Railway Research, Seoul, 2008.

Pelà, L., Aprile, A., Benedetti, A., 2009. Seismic assessment of masonry arch bridges. Engineering Structures 31 (8), 1777–1788.
Pellegrino, C., Pipinato, A., Modena, C., 2011. A simplified management procedure for bridge network maintenance. Structure and Infrastructure Engineering 7 (5), 341–351.
Pellegrino, C., Zanini, M.A., Zampieri, P., et al., 2015. Contribution of in situ and laboratory investigations for assessing seismic vulnerability of existing bridges. Structure and Infrastructre Engineering 11 (9), 1147–1162.
President of the Ministers Council, 2003. Primi elementi in materia di criteri generali per la classificazione sismica del territorio nazionale e di normative tecniche per le costruzioni in zona sismica. O.P.C.M. 3274. President of the Ministers Council, Rome.
Shinozuka, M., Feng, M., Kim, H.K., et al., 2000a. Nonlinear static procedure for fragility curve development. Journal of Engineering Mechanics 126 (12), 1287–1295.
Shinozuka, M., Feng, M., Lee, J., et al., 2000b. Statistical analysis on fragility curves. Journal of Engineering Mechanics 126 (12), 1224–1231.
Tecchio, G., da Porto, F., Zampieri, P., et al., 2012. Static and seismic retrofit of masonry arch bridges : case studies. In: 6th International Conference on Bridge Maintenance. Safety and Management, London, 2012.
Union Internationale des Chemins de fer (UIC), 2009a. Defects in Railway Bridges and Procedures for Maintenance. 778–3. UIC, Paris.
Union Internationale des Chemins de fer (UIC), 2009b. Recommendations for the Inspection, Assessment and Maintenance of Masonry Arch Bridges. 778–4. UIC, Paris.
Varum, H., Sousa, R., Delgado, W., et al., 2011. Comparative structural response of two steel bridges constructed 100 years apart. Structure and Infrastructure Engineering 7 (1), 843–855.
Zampieri, P., Cavalagli, N., Gusella, V., et al., 2018a. Collapse displacements of masonry arch with geometrical uncertainties on spreading supports. Computers and Structures 208, 118–129.
Zampieri, P., Faleschini, F., Zanini, M.A., et al., 2018b. Collapse mechanisms of masonry arches with settled springing. Engineering Structures 156, 363–374.
Zampieri, P., Simoncello, N., Pellegrino, C., 2018c. Structural behaviour of masonry arch with no-horizontal springing settlement. Frattura ed Integrità Strutturale 12 (43), 182–190.
Zampieri, P., Tecchio, G., da Porto, F., et al., 2015a. Limit analysis of transverse seismic capacity of multi-span masonry arch bridges. Bulletin of Earthquake Engineering 13 (5), 1557–1579.
Zampieri, P., Zanini, M.A., Faleschini, F., 2016. Derivation of analytical seismic fragility functions for common masonry bridge types: methodology and application to real cases. Engineering Failure Analysis 68, 275–291.
Zampieri, P., Zanini, M.A., Modena, C., 2015b. Simplified seismic assessment of multi-span masonry arch bridges. Bulletin of Earthquake Engineering 13 (9), 2629–2646.
Zampieri, P., Zanini, M.A., Zurlo, R., 2014. Seismic behaviour analysis of classes of masonry arch bridges. Key Engineering Materials 628, 136–142.

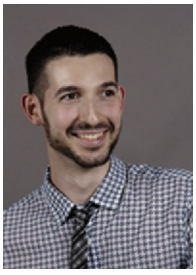

Diego Maria Barbieri is currently a PhD candidate at Norwegian University of Science and Technology, Norway. Before joining the PhD program, he obtained the 2nd level postgraduate master and specialization diploma in railway engineering at Sapienza University of Rome, Italy. He obtained his bachelor and master degree at University of Modena and Reggio Emilia, Italy. His research areas cover bridge and pavement engineering. He is particularly interested in investigating sustainable solutions for infrastructure construction.